Materials Advances

PAPER

Check for updates

Heterogeneous catalytic decomposition of hydrogen peroxide utilizing a Fe(III)-based metal–organic framework as an efficient and persistent nanozyme

Osama Abuzalat, [ID] *[a] Worood A. El-Mehalmey,[b] Hesham Tantawy, [ID] [a] Ahmad Baraka[a] and Mohamed H. Alkordi [ID] *[b]

Catalases exert their crucial role in protecting living cells from damage caused by reactive oxygen species (ROS) through effectively catalyzing hydrogen peroxide decomposition to water and oxygen. Despite the fact that naturally occurring enzymes demonstrate unparalleled activity in their natural habitat, they suffer from rapid denaturation and loss of activity under harsh conditions. Thus, it is of great interest to develop an alternative material that demonstrates intrinsic enzyme-like activity mimicking the catalase behavior, but with enhanced structural stability under industrially relevant conditions. Nanomaterials with enzyme-like activity known as "Nanozymes" have been widely used in several catalytic processes. Herein, we demonstrate the superior catalytic activity of a Fe-based metal organic framework known as MIL-53(Fe) as a cheap nanozyme generated through a facile solvothermal synthesis to catalytically mediate the H_2O_2 decomposition. The data shows that the MOF demonstrated exceptional rapid catalytic activity towards H_2O_2 decomposition without applying any heat, additionally with high recyclability without significant loss in activity for an extended number of cycles.

Introduction

Catalytic processes represent the cornerstones of many chemical transformations, ranging from those used in the industrial scale for the production of valuable feedstock and commodity products, to those occurring within living cells deriving metabolism and passage of the genetic code. The quest for an improved and optimized catalyst, designed for a specific reaction, is a multi-scale process that requires careful design and implementation. The advent of hybrid microporous solids, best represented by metal–organic frameworks (MOFs), promise unparalleled potential for their application in chemical catalysis. This is mostly due to the multitude of desirable attributes of MOFs, including their permanent porosity, which facilitates access to the active sites within the material through intriguing pore systems, associated with the underlying topology of such solids.[1] Moreover, due to their hybrid organic–inorganic composition of metal ions (or clusters), stitched through organic linkers, the chemical functionality of their molecular components can be exploited in the isolated solid. Several reports demonstrated the applicability of this design to tailor specific microporous solids for catalytic applications in the oxidation of hydrocarbons,[2] epoxidation of alkenes,[3,4] neutralization of nerve agents,[5] decontamination of organic dyes,[6–8] among others.

The seminal contribution of Yan *et al.* of the peroxidase-like Fe_3O_4 magnetic nanoparticles[9] stimulated the rapid growth of investigating similar constructs as Nanozymes.[10] Nanozymes possess several attributes that distinguish them from natural enzymes, namely their stability against denaturation under harsh reaction conditions as well as their much lower cost of preparation, purification, and storage.[10] MOFs can potentially provide a platform material capable to address the above-mentioned drawbacks of natural enzymes, yet surpass conventional nanoparticle-based catalysts due to their microporosity and hence the maximized accessibility to the true active site(s). In this study, we describe the utilization of a Fe-terephthalate MOF, known as Fe-BDC, or MIL-53(Fe), as a simple, cost-effective Nanozyme for the catalytic decomposition of hydrogen peroxide in an aqueous solution. This MOF can be readily constructed through a facile solvothermal synthesis from cheap and abundant components, where its cavities will facilitate the accessibility of target to the catalytic Fe center within the MOF structure.

Results and discussion

Fe-BDC MOF catalyst synthesis and characterization before and after H_2O_2 catalytic degradation

An iron carboxylate-based metal organic framework, named Fe-BDC MOF was successfully synthesized using a solvothermal method, as previously reported in the literature.[11]

[a] *Department of Chemical Engineering, Military Technical College, Cairo, Egypt. E-mail: osama.abuzalat@mtc.edu.eg*

[b] *Center for Materials Science, Zewail City of Science and Technology, October Gardens, Giza 12578, Egypt. E-mail: malkordi@zewailcity.edu.eg*
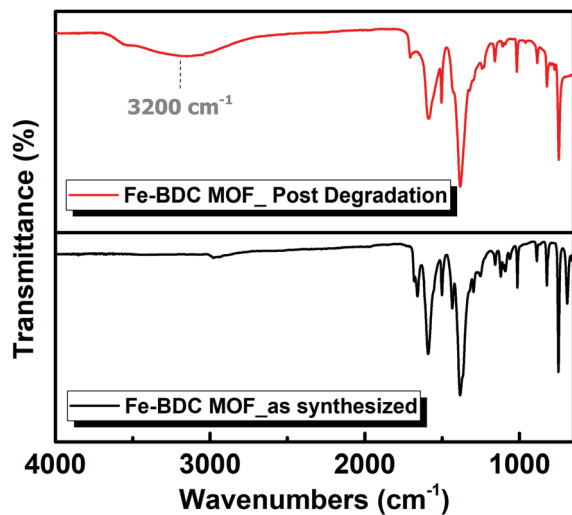
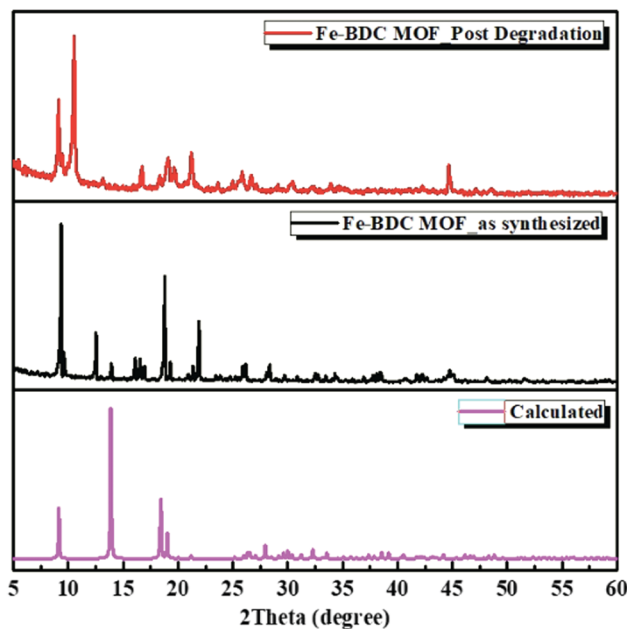Fig. 1 FTIR spectra of Fe–BDC MOF prior, and post H_2O_2 degradation.

Fig. 2 X-ray diffraction patterns of the as-synthesized Fe–BDC MOF prior and post H_2O_2 degradation. Highlighting the breathing phenomena of the MOF upon degrading the H_2O_2.

Then, several techniques were employed to characterize the MOF catalyst pre and post the catalytic degradation reaction including Fourier-transform infrared (FTIR) spectroscopy, X-ray powder diffraction (XRD), thermogravimetric analysis (TGA), X-ray photoelectron spectroscopy (XPS) and gas sorption measurements. The FT-IR spectra (Fig. 1) reveal the characteristic peaks of the isolated pristine MOF, with C=O stretching frequency at 1660 cm^{-1} as well as O–C–O asymmetric stretching frequency at 1505–1592 cm^{-1}.[12,13] Moreover, the FT-IR of the nanozyme after degrading the H_2O_2 indicated maintained functional groups associated with the organic backbone, albeit with evident transformation into different modes of Fe–CO$_2$ coordination, which can be ascribed to the formation of loosely coordinated Fe(O)$_x$ species within the material upon oxidation with H_2O_2. Moreover, significant absorption at ~3200 cm^{-1} indicates the presence of –OH terminated species, most likely Fe–OH/OH$_2$ from the decomposed H_2O_2.[14] To assess the crystallinity and phase purity of the as-synthesized Fe–BDC MOF, X-ray powder diffraction (XRD) was recorded for the MOF before adding H_2O_2, which demonstrated characteristic peaks that well matched with those reported for Fe–BDC MOF in a previous literature.[15] Thus, it confirmed that the pure Fe–BDC MOF was prepared successfully under the used conditions. However, after the successive degradation of H_2O_2, it could be observed that the Fe–BDC MOF XRD pattern degraded slightly amorphized, and the peaks became broader. It seems that the degradation process impacted the crystallinity of the MOF, leading to a slight reduction in the framework crystallinity and structural alterations without the full loss of crystallinity.[16,17] As the common major diffraction peaks (Fig. 2) at 2θ = 9.24°, 13.6°, 18.3°, 19.2°, 21.3°, 25.8°, 30.6° and 44.7° were maintained after the catalytic reaction as well as being consistent with the simulated ones,[11,15,18] they indicated the survivability of Fe–BDC MOF even under a harsh degradation environment. However, the disappearance of the peaks at 2θ = 12.4°, 13.9°, 16.1°, and 21.9° and the appearance of a new

strong peak at 2θ = 10.8° and other weak ones at 2θ = 13.2°, 18.4°, 19.7° and 26.7° after H_2O_2 degradation may indicate the notable breathing behavior with an adapted pore opening as a result of a possible solvent exchange or a H_2O_2 adsorption process during the catalytic process.[19–21]

This phenomenon may be attributed to the different forces imposed on the framework during the H_2O_2 degradation accompanied by the solvent/guest exchange,[17,22] resulting in Fe–BDC pore size profile swapping.[19,23] The switching of disordered guest molecules significantly affects the volume of the unit cell and leads to disordering within the structure, which results from the diverse coordination interactions with the MOF metal nodes.[24,25] Moreover, the notable shifting in some of the main diffraction peaks may be due to the dehydration of some crystalline domains during the oxidation process, which led to a minor deflection of adjacent domains and increased the number of crystallite orientations in some portion of the sample. Thermogravimetric analysis (TGA) was conducted under N_2 atmosphere to study the thermal stability of the MOF catalyst before and after the degradation (Fig. 3). The TGA pattern of Fe–BDC MOF shows that a continuous weight loss commences around 200 °C and continues up to ~330 °C, which corresponds to the loss of coordinated water molecules. Above 330 °C, the decomposition of the BDC^{2-} is followed by conversion of the Fe species into Fe(O)$_x$.

After exposure to H_2O_2, TGA indicated an additional weight loss step at 500 °C, which was not present in the pristine MOF, most likely a metal–carbonate decomposition step, which is in agreement with the XPS assignment on the partial formation of metal–carbonate species upon H_2O_2 exposure.

As shown in Fig. 4, the XPS survey spectrum of the obtained Fe–BDC MOF before and after treatment with H_2O_2 confirmed
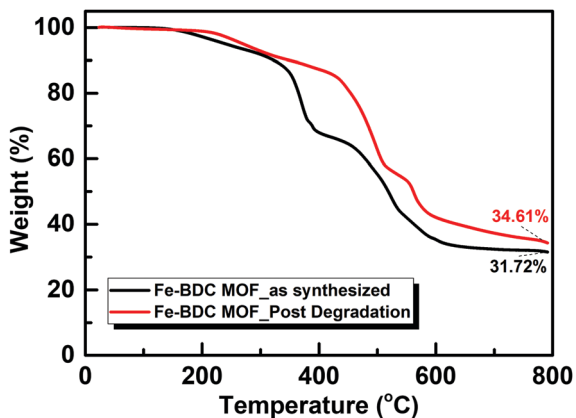
Fig. 3 TGA of the as-synthesized Fe-BDC MOF prior, and post H_2O_2 degradation.

Table 1 XPS Analysis showing atomic % for the several elements in the MOF (as-synthesized) and (post degradation)

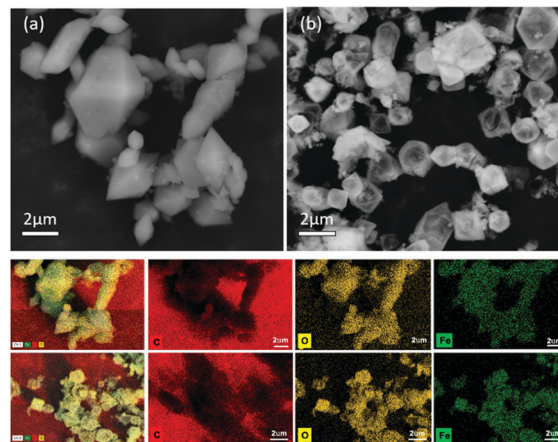| Element (atomic %)	C	O	Fe
Fe-BDC MOF (as-synthesized)	59.95	26.83	4.6
Fe-BDC MOF (post degradation)	30.24	48.45	15.67

Fig. 5 SEM images of the as-synthesized Fe-BDC MOF (a) prior, and (b) post H_2O_2 degradation. The panel below shows the EDX elemental mapping of the as-synthesized MOF (top row) and that after catalytic reaction (below) showing the homogeneous distribution of the elements (labeled images) throughout the sample.

the presence of Fe, C, and O elements on the surface of the sample, albeit with the increased Fe, O/C ratio in the H_2O_2-treated sample, as shown in Table 1. For the pristine sample, the C 1s XPS spectrum demonstrated a peak at 284.88 eV assigned to C–C/C=C of the ligands, a small shoulder at 286.28 eV that could be assigned to oxygenated C–O species, and a peak at 288.74 eV characteristic of O–C=O groups of the linkers.[26] The O 1s spectrum can be de-convoluted into three peaks at 530.5 eV assigned to Fe–(OH) groups, 531.8 eV attributed to the C=O in carboxylate groups, and 533.3 eV attributed to the adsorbed water molecules on the surface of the material. The XPS spectrum of Fe 2p showed a peak with a binding energy of 711.68 eV assigned to $Fe2p_{3/2}$ of Fe(III) and 725.48 eV

assigned to $Fe2p_{1/2}$ of Fe(III).[13,15] After adding the H_2O_2, the XPS survey spectrum as well as the EDX maps were obtained (Fig. 5) and confirmed the presence of Fe, C, and O elements on the surface of the sample.

However, the most significant change in the MOF catalyst is in the changes in the C 1s spectrum, where the MOF exhibits strong peaks for metal-coordinated carbonate carbon (288.99 eV), presumably produced through the partial oxidation of the MOF organic backbone by the combined action of the H_2O_2 and the catalytic Fe center.[14]

Scanning electron microscopy (SEM) was also utilized to characterize the MOF before and after the catalytic decomposition of H_2O_2. The SEM images, Fig. 5, indicated a change in the topography of the MOF, resulting from the partial deformation of the MOF crystallite backbone after being exposed to the H_2O_2 oxidant.

Probing the catalytic degradation efficiency and recyclability of Fe-BDC MOF against H_2O_2

The addition of Fe-BDC MOF to H_2O_2 aqueous solution revealed its excellent performance as a Nanozyme for the catalytic decomposition of H_2O_2. Remarkably, the addition of 200 mg of Fe-BDC Nanozyme to 6 g of the 47 wt% H_2O_2 aqueous solution was sufficient to result in 57% weight loss of the aqueous solution in only two minutes without even applying any heat. Moreover, increasing the amount of MOF added to the hydrogen peroxide solution shortened the time required for reaching the same degradation efficiency, where adding 0.5 g of
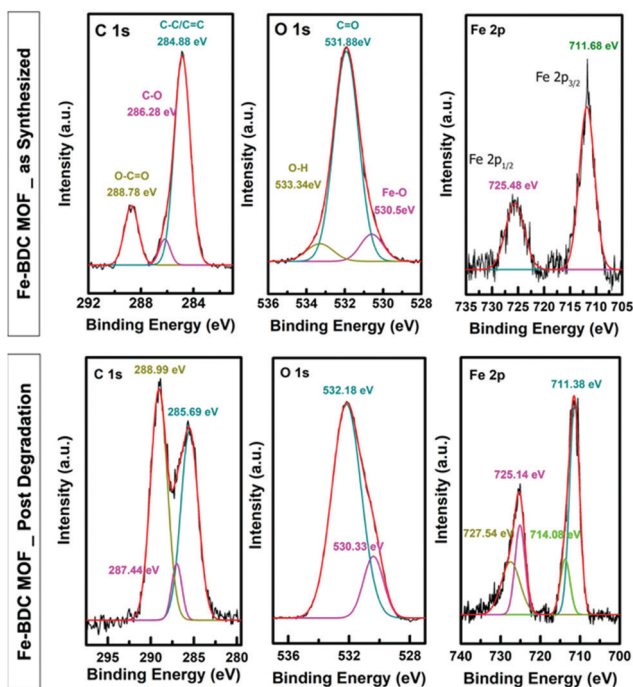

Fig. 4 XPS detailed line scans of the as-synthesized Fe-BDC MOF (top), the MOF post degradation (bottom).
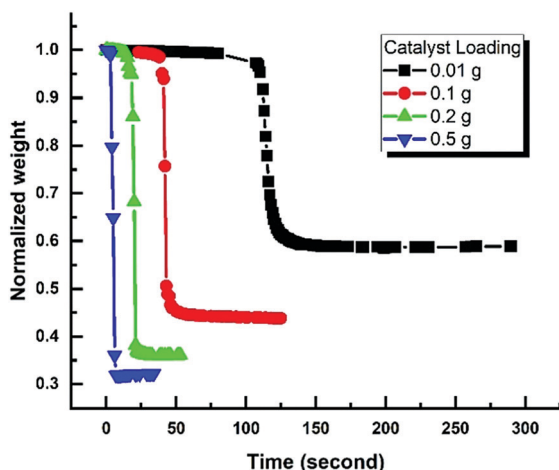
Fig. 6 Degradation capabilities of different weights of Fe-BDC MOF against H_2O_2.

MOF was sufficient to induce a significant weight loss of the sample through the catalytic degradation of H_2O_2 accompanied by an exothermic reaction and water evaporation, altogether very rapidly within 10 seconds of mixing the catalyst with the peroxide solution (Fig. 6). The data recorded shown indicates the weight loss due to the evolution and escape of O_2 gas as a function of time after introducing the catalyst to the peroxide solution. As the experiments were done in an open vessel, unavoidable loss of moisture occurred as the reaction was highly exothermic.

Interestingly, retrieving the Nanozyme through centrifugation and assessing its recyclability for 6 consecutive cycles did not show any noticeable decay in its catalytic activity, marking an industrially applicable Nanozyme towards H_2O_2 decomposition for oxygen evolution (Fig. 7). It is worth mentioning here that the weight loss calculation was very comparable to the iodometric titration for H_2O_2 determination after its catalytic degradation over Fe-BDC.
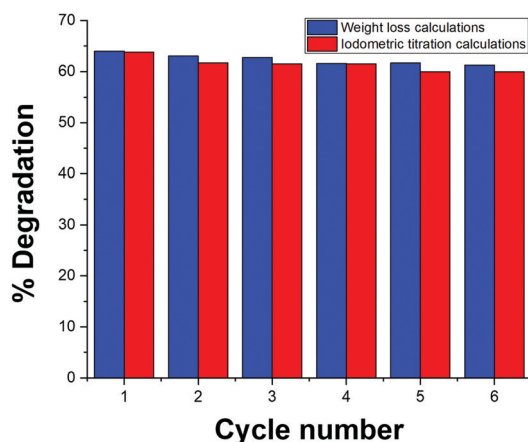

Fig. 7 Investigating the recyclability capabilities of Fe-BDC MOF (0.2 g) towards H_2O_2 degradation.

Conclusion

In conclusion, we presented the utilization of the Fe-based MOF (MIL-53(Fe)) as a nanozyme for the catalytic degradation of hydrogen peroxide. The MOF nanozyme was prepared through a simple solvothermal reaction, making it scalable for industrial applications. Furthermore, the MOF demonstrated an excellent catalytic performance against H_2O_2 in only a few seconds, with no detectable loss of activity even after six consecutive cycles. Moreover, the MOF exhibited a notable breathing behavior with an adapted pore opening as a result of a possible H_2O_2 adsorption during the catalytic process.

Experimental

Caution

H_2O_2 with relatively high concentration is highly corrosive and the reaction should be carried out in an open vessel wearing protective body equipment and face shield in a properly ventilated hood.

Materials

All reagents were used as received without further purification. Solvents and common chemicals were purchased from Sigma-Aldrich or Fisher Scientific-UK. Iron chloride ($FeCl_3 \cdot 6H_2O$, 98%, Sigma Aldrich), 1,4 benzene dicarboxylic acid (H_2BDC, 98%, Sigma Aldrich), and *N,N*-dimethylformamide (DMF, 98%, Sigma Aldrich). Absolute ethanol, acetone (all from Alfa Aesar)), H_2O_2, (47%, Sigma Aldrich), and deionized water were used for washing purposes. Potassium iodide (KI, 99%, Sigma Aldrich), ammonium molybdate (99%, Sigma Aldrich), sulfuric Acid (H_2SO_4, Alfa Aesar), sodium thiosulfate ($Na_2S_2O_3$, 98% Sigma Aldrich), and starch indicator for H_2O_2 iodometric titration purposes were used.

Infra-red absorption spectra were recorded on a Thermo Scientific Nicolet is-10. X-ray powder diffractions were taken on a Shimadzu XD-l X-Ray powder diffractometer. SEM/EDX images were taken on a Zeiss EVO-10 microscope for the examination of the surface morphology and the elemental composition. The X-ray photoelectron spectrum (XPS) measurements were performed using a K-ALPHA XPS system (Themo Fisher Scientific, USA) with a monochromatic Al-K$_\alpha$ source operated at 15 keV.

Methods

Preparation of Fe-BDC

Samples were synthesized through the sequential addition of $FeCl_3 \cdot 6H_2O$ (0.27 g, 1 mmol), and 1,4-benzenedicarboxylic acid (H_2BDC) (0.166 g, 1 mmol), and glacial acetic acid (1 mL) into a beaker, followed by the addition of *N,N*-dimethylformamide (DMF) (20 mL) under stirring until the reagents were completely dissolved. The mixture was then transferred into a scintillation vial, which was sealed and placed in isothermal oven at 100 °C for 6 h. The resulting powder was recovered by

centrifugation at 6000 rpm for 30 min, and rinsed three times with DMF, acetone, ethanol, and water. Finally, the recovered crystals were placed into an oven set at 140 °C to dry overnight.

H_2O_2 degradation and recyclability investigation

In a typical degradation trial, 6 mL of 47% H_2O_2 aqueous solution containing 0.2 grams of Fe-BDC MOF powder was left at room temperature. After one second, the degradation of H_2O_2 was monitored through recording the weight loss using a digital scale. The degradation efficiency of the MOF was tested using the same volume of H_2O_2 and varying the weight of the MOF ranging from 0.01 to 0.5 grams. For recyclability, the MOF powder was isolated from the mixture by centrifugation at 6000 rpm for 30 min, washed with 50 mL DI water, and then dried at 120 °C for 2 h between each cycle. The H_2O_2 degradation and washing steps were repeated for 6 consecutive cycles.

Conflicts of interest

There are no conflicts to declare.

Acknowledgements

References

1 D. Yang and B. C. Gates, Catalysis by metal organic frameworks: Perspective and suggestions for future research, *ACS Catal.*, 2019, **9**(3), 1779–1798, DOI: **10.1021/acscatal. 8b04515**.

2 A. Dhakshinamoorthy, A. M. Asiri and H. Garcia, Metal–organic frameworks as catalysts for oxidation reactions, *Chem. – Eur. J.*, 2016, **22**(24), 8012–8024, DOI: **10.1002/ chem.201505141**.

3 J. W. Brown, Q. T. Nguyen, T. Otto, N. N. Jarenwattananon, S. Glöggler and L. S. Bouchard, Epoxidation of alkenes with molecular oxygen catalyzed by a manganese porphyrin-based metal–organic framework, *Catal. Commun.*, 2015, **59**, 50–54, DOI: **10.1016/j.catcom.2014.09.040**.

4 K. Yuan, T. Song, D. Wang, Y. Zou, J. Li, X. Zhang, Z. Tang and W. Hu, Bimetal–organic frameworks for functionality optimization: MnFe-MOF-74 as a stable and efficient catalyst for the epoxidation of alkenes with H_2O_2, *Nanoscale*, 2018, **10**(4), 1591–1597, DOI: **10.1039/c7nr08882e**.

5 K. O. Kirlikovali, Z. Chen, T. Islamoglu, J. T. Hupp and O. K. Farha, Zirconium-based metal–organic frameworks for the catalytic hydrolysis of organophosphorus nerve agents, *ACS Appl. Mater. Interfaces*, 2020, **12**(13), 14702–14720, DOI: **10.1021/acsami.9b20154**.

6 Alamgir, K. Talha, Y. J. Wang, R. Ullah, B. Wang, L. Wang, W. Wu, S. Chen, L. H. Xie and J. R. Li, Construction of a mixed ligand MOF as ''Green Catalyst'' for the photocatalytic degradation of organic dye in aqueous media, *RSC Adv.*, 2021, **11**(38), 23838–23845, DOI: **10.1039/d1ra02994k**.

7 A. H. Ibrahim, R. R. Haikal, R. S. Eldin, W. A. El-Mehalmey and M. H. Alkordi, The role of free-radical pathway in catalytic dye degradation by hydrogen peroxide on the Zr-based UiO-66-NH$_2$ MOF, *ChemistrySelect*, 2021, **6**(42), 11675–11681, DOI: **10.1002/slct.202102955**.

8 Z. Wu, X. Yuan, J. Zhang, H. Wang, L. Jiang and G. Zeng, Photocatalytic decontamination of wastewater containing organic dyes by metal–organic frameworks and their derivatives, *ChemCatChem*, 2017, **9**(1), 41–64, DOI: **10.1002/ cctc.201600808**.

9 L. Gao, J. Zhuang, L. Nie, J. Zhang, Y. Zhang, N. Gu, T. Wang, J. Feng, D. Yang and S. Perrett, *et al.*, Intrinsic peroxidase-like activity of ferromagnetic nanoparticles, *Nat. Nanotechnol.*, 2007, **2**(9), 577–583, DOI: **10.1038/nnano. 2007.260**.

10 D. Jiang, D. Ni, Z. T. Rosenkrans, P. Huang, X. Yan and W. Cai, Nanozyme: New horizons for responsive biomedical applications, *Chem. Soc. Rev.*, 2019, **48**(14), 3683–3704, DOI: **10.1039/c8cs00718g**.

11 T. R. Whitfield, X. Wang, L. Liu and A. J. Jacobson, Metal–organic frameworks based on iron oxide octahedral chains connected by benzenedicarboxylate dianions, *Solid State Sci.*, 2005, **7**(9), 1096–1103, DOI: **10.1016/j.solidstate sciences.200503.007**.

12 X. Lou, H. Hu, C. Li, X. Hu, T. Li, M. Shen, Q. Chen and B. Hu, Capacity control of ferric coordination polymers by zinc nitrate for lithium-ion batteries, *RSC Adv.*, 2016, **6**(89), 86126–86130, DOI: **10.1039/c6ra17608a**.

13 W. Mei, D. Li, H. Xu, J. Zan, L. Sun, Q. Li, B. Zhang, Y. Wang and D. Xia, Effect of electronic migration of MIL-53(Fe) on the activation of peroxymonosulfate under visible light, *Chem. Phys. Lett.*, 2018, **706**, 694–701, DOI: **10.1016/ j.cplett.2018.07.020**.

14 T. T. Quang, N. X. Truong, T. H. Minh, N. N. Tue and G. T. P. Ly, Enhanced photocatalytic degradation of MB under visible light using the modified MIL-53(Fe), *Top. Catal.*, 2020, **63**(11–14), 1227–1239, DOI: **10.1007/s11244-020-01364-2**.

15 T. A. Vu, G. H. Le, C. D. Dao, L. Q. Dang, K. T. Nguyen, Q. K. Nguyen, P. T. Dang, H. T. K. Tran, Q. T. Duong and T. V. Nguyen, *et al.*, Arsenic removal from aqueous solutions by adsorption using novel MIL-53(Fe) as a highly efficient adsorbent, *RSC Adv.*, 2015, **5**(7), 5261–5268, DOI: **10.1039/ c4ra12326c**.

16 A. M. Ebrahim and T. J. Bandosz, Ce(III) doped Zr-based MOFs as excellent NO2 adsorbents at ambient conditions, *ACS Appl. Mater. Interfaces*, 2013, **5**(21), 10565–10573, DOI: **10.1021/am402305u**.

17 R. A. Dodson, A. G. Wong-Foy and A. J. Matzger, The metal–organic framework collapse continuum: Insights from two-dimensional powder X-ray diffraction, *Chem. Mater.*, 2018, **30**(18), 6559–6565, DOI: **10.1021/acs.chemmater. 8b03378**.

18 J. O. Hsieh, K. J. Balkus, J. P. Ferraris and I. H. Musselman, MIL-53 frameworks in mixed-matrix membranes, *Microporous Mesoporous Mater.*, 2014, **196**, 165–174, DOI: **10.1016/j.micromeso.2014.05.006**.

19 A. S. Munn, A. J. Ramirez-Cuesta, F. Millange and R. I. Walton, Interaction of methanol with the flexible metal–organic framework MIL-53(Fe) observed by inelastic neutron scattering, *Chem. Phys.*, 2013, **427**, 30–37, DOI: **10.1016/j.chemphys.2013.05.017**.

20 N. Guillou, F. Millange and R. I. Walton, Rapid and reversible formation of a crystalline hydrate of a metal–organic framework containing a tube of hydrogen-bonded water, *Chem. Commun.*, 2011, **47**(2), 713–715, DOI: **10.1039/c0cc03882b**.

21 H. Reinsch, R. S. Pillai, R. Siegel, J. Senker, A. Lieb, G. Maurin and N. Stock, Structure and properties of Al-MIL-53-ADP, a breathing MOF based on the aliphatic linker molecule adipic acid, *Dalton Trans.*, 2016, **45**(10), 4179–4186, DOI: **10.1039/c5dt03510d**.

22 D. Zhang, Y. Guan, E. J. M. Hensen, T. Xue and Y. Wang, Tuning the hydrogenation activity of Pd NPs on Al-MIL-53 by linker modification, *Catal. Sci. Technol.*, 2014, **4**(3), 795–802, DOI: **10.1039/c3cy00910f**.

23 S. Bourrelly, B. Moulin, A. Rivera, G. Maurin, S. Devautour-Vinot, C. Serre, T. Devic, P. Horcajada, A. Vimont and G. Clet, *et al.*, Explanation of the adsorption of polar vapors in the highly flexible metal organic framework MIL-53(Cr), *J. Am. Chem. Soc.*, 2010, **132**(27), 9488–9498, DOI: **10.1021/ja1023282**.

24 W. Wong-Ng, H. G. Nguyen, L. Espinal, D. W. Siderius and J. A. Kaduk, Powder X-ray structural studies and reference diffraction patterns for three forms of porous aluminum terephthalate, MIL-53(A1), *Powder Diffr.*, 2019, **34**(3), 216–226, DOI: **10.1017/S0885715619000460**.

25 S. Couck, J. F. M. Denayer, G. V. Baron, T. Rémy, J. Gascon and F. Kapteijn, An amine-functionalized MIL-53 metal–organic framework with large separation power for CO_2 and CH_4, *J. Am. Chem. Soc.*, 2009, **131**(18), 6326–6327, DOI: **10.1021/ja900555r**.

26 G. Greczynski and L. Hultman, The same chemical state of carbon gives rise to two peaks in X-ray photoelectron spectroscopy, *Sci. Rep.*, 2021, **11**(1), 1–5, DOI: **10.1038/s41598-021-90780-9**.